

## GENERATION OF SUBURBAN TERRAIN INFLOW CONDITIONS FOR LARGE EDDY SIMULATIONS

Yi-Chao Li<sup>1</sup>, Chii-Ming Cheng<sup>2</sup>, Fuh-Min Fang<sup>3</sup>, Chen-Hsin Chang<sup>4</sup>, Yuan-Lung Lo<sup>5</sup>

<sup>1</sup>*Research Fellow, Wind Engineering Research Center, Tamkang University, New Taipei City, 251, Taiwan,  
liyichao223@gmail.com*

<sup>2</sup>*Professor, Department of Civil Engineering, Tamkang University, New Taipei City, 251, Taiwan,  
cmcheng@mail.tku.edu.tw*

<sup>3</sup>*Professor, Department of Civil Engineering, National Chung Hsing University,  
Taichung, 250, Taiwan, fmfang@nchu.edu.tw*

<sup>4</sup>*Professor, Department of Civil Engineering, Tamkang University, New Taipei City, 251, Taiwan,  
cc527330@mail.tku.edu.tw*

<sup>5</sup>*Assistant Professor, Department of Civil Engineering, Tamkang University, New Taipei City, 251, Taiwan,  
yllo@mail.tku.edu.tw*

### ABSTRACT

To generate the suitable atmospheric boundary layer inlet for large eddy simulation, one of the most important techniques of computational wind engineering, the MDSRFG (modified discretizing and synthesizing random flow generation) was selected to numerically generate the inhomogeneous and anisotropic turbulence boundary layer in this paper. A weakly-compressible-flow method along with the large eddy simulation (LES) was utilized to reproduce the unsteady flow field. Parameters, such as mean wind speeds, turbulence intensities and turbulence integral scales from fully-developed turbulent boundary layer flow were provided by well-established wind tunnel tests. Furthermore, coherence between any two fluctuating wind speeds was taken into account for a more compact simulation of inflow. It was indicated that the method works well as a suburban turbulence boundary layer generator by comparing the characteristics of mean wind speed profiles, turbulence intensity profiles and power spectra at the centerline of several positions along longitudinal direction from wind tunnel tests.

**KEYWORDS:** COMPUTATION FLUID DYNAMIC, TURBULENCE BOUNDARY LAYER, LARGE EDDY SIMULATION

### Introduction

Reproduction of the real turbulence flow field is one of the most important issues in computational wind engineering. The discretizing and synthesizing random flow generation (DSRFG) method, a new inflow turbulence generation method developed by Huang et al. (2010), is adopted to produce an inlet fluctuating velocity field that meet specific spectrum. Castro et al. (2011) modified the DSRFG (MDSRFG) method based on DSRFG, preserving the statistical quantities at the inlet part of the full domain and keeping independent of number of points for simulating target spectrum.

The aim of this study is to generate a suitable inlet condition of suburban terrain for LES simulation and evaluate the time and spatial correlation as parameters. The invariant turbulence intensity profile and wind speed spectra in the alongwind direction are examined to ensure successful reproduction of the simulated field from the upstream distance to the testing object.

## Methodology

To simulate the unsteady flow field, a weakly-compressible-flow method (Song and Yuan, 1988) along with a sub-grid scale turbulence model (Smagorinsky, 1963) is employed. A finite-volume method is adopted to calculate and then update the fluxes within each elapsed time based on an explicit predictor-corrector scheme (MacCormack, 1969). During the computation process, the time increment is limited by the CFL criterion (Courant et al., 1967).

$$\frac{\partial p}{\partial t} + \nabla \cdot (\vec{k}\vec{V}) = 0 \quad (1)$$

$$\frac{\partial \vec{V}}{\partial t} + \vec{V} \cdot \nabla \vec{V} = -\nabla \frac{p}{\rho} + \nabla \cdot [(\nu + \nu_t)\nabla \vec{V}] \quad (2)$$

Derivation of the MDSRFG method and associated validation researches are given by Castro et al. (2011). A brief formulation of the method is presented as below.

$$U(x, t) = \sum_{m=1}^M \sum_{n=1}^N \left[ p_i^{m,n} \cos \left( \tilde{k}_j^{m,n} \tilde{x}_j + \omega_{m,n} \frac{t}{\tau_0} \right) + q_i^{m,n} \sin \left( \tilde{k}_j^{m,n} \tilde{x}_j + \omega_{m,n} \frac{t}{\tau_0} \right) \right], \quad (3)$$

where

$$p_i^{m,n} = \text{sign}(r_i^{m,n}) \sqrt{\frac{4c_i}{N} E_i(k_m) \Delta k_m \frac{(r_i^{m,n})^2}{1 + (r_i^{m,n})^2}}, \quad (4)$$

$$q_i^{m,n} = \text{sign}(r_i^{m,n}) \sqrt{\frac{4c_i}{N} E_i(k_m) \Delta k_m \frac{1}{1 + (r_i^{m,n})^2}}, \quad (5)$$

with  $\omega_{m,n} \in N(0, 2\pi f_m)$ ,  $r_i^{m,n}$  is a three dimensional normal distributed random number with  $\mu_r = 0$  and  $\sigma_r = 0$ .  $c_i = 0.5\bar{U}$  and  $\bar{U}$  is the mean wind speed.  $\tilde{x} = x/L_s$  and  $L_s = \theta_1 \sqrt{L_u^2 + L_v^2 + L_w^2}$  is the scaling factor for spatial correlation.  $\tau_0 = \theta_2 L_s / \bar{U}$  is a parameter introduced to allow some control over the time correlation.  $\tilde{k}^{m,n} = \mathbf{k}^{m,n} / k_0$  is the three dimensional distribution on the sphere of inhomogeneous and anisotropic turbulence.

## Inflow specification

The inhomogeneous anisotropic turbulent conditions of the suburban terrain field were created in this study. The spectra of the three principal velocity components are described by von Kármán models, i.e.,

$$S_u(f) = \frac{4(I_u \bar{U})^2 (L_u / \bar{U})}{\left[ 1 + 70.8 (f L_u / \bar{U})^2 \right]^{5/6}}, \quad (6)$$

$$S_v(f) = \frac{4(I_v \bar{U})^2 (L_v / \bar{U}) \left[ 1 + 188.4 (2f L_v / \bar{U})^2 \right]}{\left[ 1 + 70.8 (2f L_v / \bar{U})^2 \right]^{11/6}}, \quad (7)$$

$$S_w(f) = \frac{4(I_w \bar{U})^2 (L_w / \bar{U}) \left[ 1 + 188.4 (2fL_w / \bar{U})^2 \right]}{\left[ 1 + 70.8 (2fL_w / \bar{U})^2 \right]^{11/6}} \quad (8)$$

where  $I$  and  $L$  are turbulence intensity and length scale respectively.

All the given parameters obtained from TKU BL1 wind tunnel experiments are shown in Fig. 1. The mean wind speed profile is set to follow the power law with  $\alpha=0.25$ . The longitudinal turbulence intensity profile is set to  $I_u = 0.3 - 0.26(z/\delta)^{0.35}$ , and the turbulence intensity in the other two directions are assumed as  $I_v = 0.75I_u$  and  $I_w = 0.5I_u$  respectively. The longitudinal length scale ( $L_u$ ) profile is regressed to a polynomial of degree 6, and  $L_v$  and  $L_w$  are both assumed as  $0.5L_u$ .

### Parameter adjustment

The auto-correlation function can be computed by some mathematical manipulation(Huang et al.):

$$\overline{u(x,t)u(x,t+\tau)} = \frac{2c}{N} \sum_{m=1}^M \sum_{n=1}^N E(k_m) \Delta k_m \cos\left(\frac{\tau}{\tau_0} \omega_{m,n}\right) \quad (9)$$

noting that, the auto-correlation coefficients are dominated by frequency segments ( $\Delta k_m$ ) and time correlation parameter  $\theta_2$ . The discretizing segments  $M=2000$  are chosen because that the calculating efficiency and the auto-correlation coefficients change indistinctly after  $M>2000$  (shown in Fig. 2(a)). According to the auto-correlation coefficients obtained from wind tunnel experiments, time correlation parameter  $\theta_2$  can be confirmed. Fig. 2(b) shows the auto-correlation coefficients is well represented with  $\theta_2 = 0.2$ .

An expression for the spatial correlation can be obtained in an analogous way:

$$\overline{u(x,t)u(x',t)} = \sum_{m=1}^M \sum_{n=1}^N \frac{2}{N} E(k_m) \cos\left[\tilde{k}_j^{m,n} \frac{(x'_j - x_j)}{L_s}\right] \quad (10)$$

The above equation shows that the spatial correlation is controlled by  $L_s$ , therefore the  $\theta_2$  adjustment is the preliminary work in this step. However, it is unusual to estimate the complete spatial correlation coefficients in the wind tunnel therefore there is no theoretical equation for reference. In this study the square root of coherence (also known as narrow-band cross-correlation), proposed by Davenport (1968), is adopted to be the target spectra:

$$Coh = e^{-\hat{f}}, \quad \hat{f} = \frac{n \left[ C_z^2 (z_1 - z_2)^2 + C_y^2 (y_1 - y_2)^2 \right]^{1/2}}{0.5 [U(z_1) + U(z_2)]} \quad (11)$$

where  $y_1, y_2, z_1, z_2$  are the coordinate on y-z plane.  $C_y$  and  $C_z$  are the exponential decay coefficient in horizontal and vertically direction, respectively.  $C_z = 10$  and  $C_y = 16$  are suggested by Davenport.

In the boundary layer flow field, the main variation of turbulence intensity and turbulence integral length scale profile are all along the vertical direction, therefore the

adjustment of  $\theta_2$  is based on fitting the vertical coherences to near the theoretical function first. In Fig. 5 the u-component coherences are obtained at half of boundary layer thickness ( $z/\delta = 0.5$ ) with  $\Delta z/\delta = 0.02$ . When  $\theta_1 = 25$ , the coherence values are higher than target spectra. As  $\theta_1$  decreases the coherence decreases. The coherences of simulation with  $\theta_1 = 5.5$  fit well to target spectra. Fig. 6 and Fig. 7 show the coherence values at horizontal and cross-sectional (horizontal and vertical) positions when  $\theta_1 = 5.5$ . Also, the simulation patterns are close to target spectra. Hence, the spatial correlation results from simulation with  $\theta_1 = 5.5$  are consistent with theoretical values.

Lastly, we considered the synthesizing efficiency, spatial correlation and time correlation for suburban terrain, and then integrated all MDSRFG parameters into Table 1.

### **Inflow Synthesizing**

The turbulence flow field is generated by MDSRFG with sampling frequency, say 500Hz. The total sampling points are 32768. By comparing coherences of simulating and experiment results, the spatial correlation parameter  $\theta_1$  was obtained. Then the time correlation parameter  $\theta_2$  is derived using the auto-correlation on wind tunnel experiments.

Fig. 6 shows the mean wind speed and turbulence intensity profiles at central line of the inflow generated by MDSRFG. Mean wind speed profile of simulation fit well to the set target, representing that the mean speeds are very close to 0. Further, the turbulence intensity profiles in three principal directions of simulation also correspond to the set one.

Fig. 7 illustrates the power spectra of simulation results at three heights of  $z/\delta = 0.1, 0.5$  and  $0.75$  for the u-, v- and w-components of velocity fluctuations obtained are compared to von Kármán spectra. The simulated spectra fit fairly well to the target spectra in three principal directions, indicating that the anisotropy of the spectra is well represented by the proposed method.

### **Numerical Simulation**

In this research, an open terrain model is established to investigate the turbulence variation along the longitudinal direction, and the inflow turbulence is generated by MDSRFG method. The longitudinal (x), horizontal (y), and vertical (z) lengths of computational domain are 15 m, 2 m and 1 m (same as boundary layer thickness) respectively. In consideration of computational resource and efficiency, the first point near the wall surface of the domain is set to be  $0.005 \delta$ , which is also applied at inflow due to drastic change in the flow velocity. The total computational grid points are  $251 \times 51 \times 81$ .

Fig. 8 shows the mean velocity and turbulent intensity profile variation of u-component along the longitudinal direction. As the results of Fig. 8(b), all of the mean velocity profiles follow the power law. The turbulence intensity weakens significantly when  $x/\delta > 0.1$  (Fig. 8(b)) from 25 % to 18 % in the nearest wall. A survey of power spectra at 4 heights ( $z/\delta = 0.3, 0.4, 0.6, 0.8$ ) is depicted in Fig. 9. In general, the turbulence energy is preserved well at low frequency ( $f_s < 80$  Hz), but decays at high frequencies. As the height level rises,  $f_s$  increases and the energy decay is smaller.

### **Conclusions**

In this research, the MDSRFG is adopted to generate the inlet boundary condition of the suburban terrain flow field by numerical simulation. The mean wind speed profile, turbulence intensity profiles and power spectra of velocity fluctuations of simulation results fit fairly well to targets. The parameters of spatial and time correlations are adjusted by wind tunnel results and theoretical equations to prove that the MDSRFG method can be an effective numerical tool for generating a spatially correlated atmospheric boundary layer flow field. However, the turbulent energy at high frequencies decays along the x direction. Through

adopting finer grid point, or a suitable inflow profile of turbulent intensity and length scale, the turbulent energy may be conserved.

## References

- Sminov, A., Shi, S. and Celik, I. (2001), "Random Flow Generation Technique for Large Eddy Simulation and Particle-Dynamics Modeling," *Journal of Fluids Engineering*, Vol. 123, 359-371.
- Huang, S. H., Li, Q. S. and Wu, J. R. (2010), "A General Inflow Turbulence Generator for Large Eddy Simulation," *Journal of Wind Engineering and Industrial Aerodynamic*, Vol.98, 600-617.
- Castro, H. G., Paz, R. R., and Sonzogni, V. E. (2011), "Generation of Turbulence Inlet Velocity Conditions for Large Eddy Simulation," *Mecánica Computacional*, Vol. XXX, 2275–2288.
- Song, C., Yuan, M. (1988), "A weakly compressible flow model and rapid convergence methods," *Journal of Fluids Engineering*, 110(4), 441-455.
- MacCormack, R. (1969), "The effect of viscosity in hyper-velocity impact cratering," AIAA paper 69-354.
- Smagorinsky, J., 1963. General circulation experiments with primitive equations. *Month Weather Review* 91(3), 99-164.
- Courant, R., Friedrich, K., Lewy, H. (1967), "On the partial differential equations of mathematical physics," *IBM Journal*, 11(2), 215-234.
- Davenport, A. G. (1968), "The dependence of wind load upon Meteorological Parameter," in *Proceedings of the International Research Seminar on Wind Effects on Buildings and Structures*, University of Toronto Press, Toronto, pp. 19-82.

Table 1 : MDSRFG Parameters for suburban terrain

N	M	$K_0$	$\theta_1$	$\theta_2$
100	2000	0.01	5.5	0.2

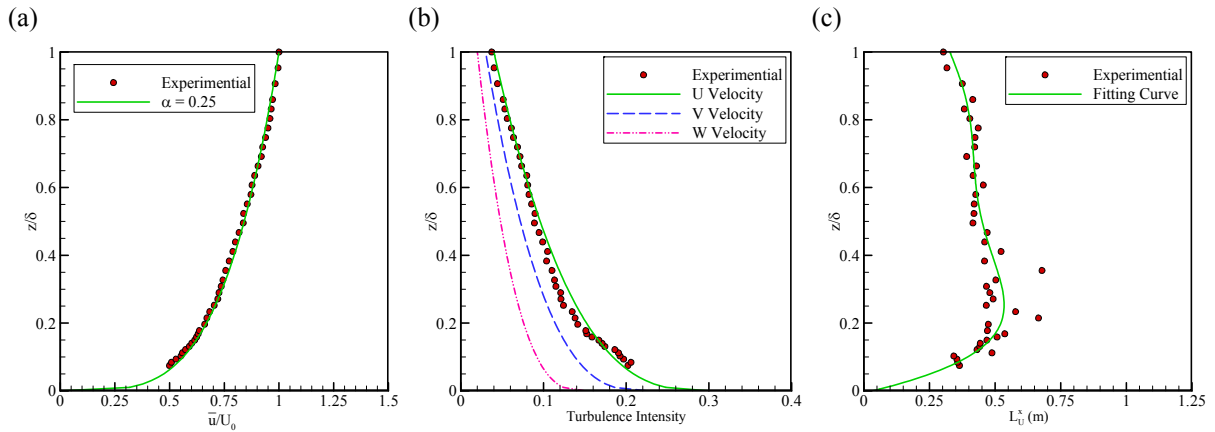


Fig.1 Vertical profiles of Inlet condition (a) mean wind speed, (b) turbulence intensity and (c) integral length scale.

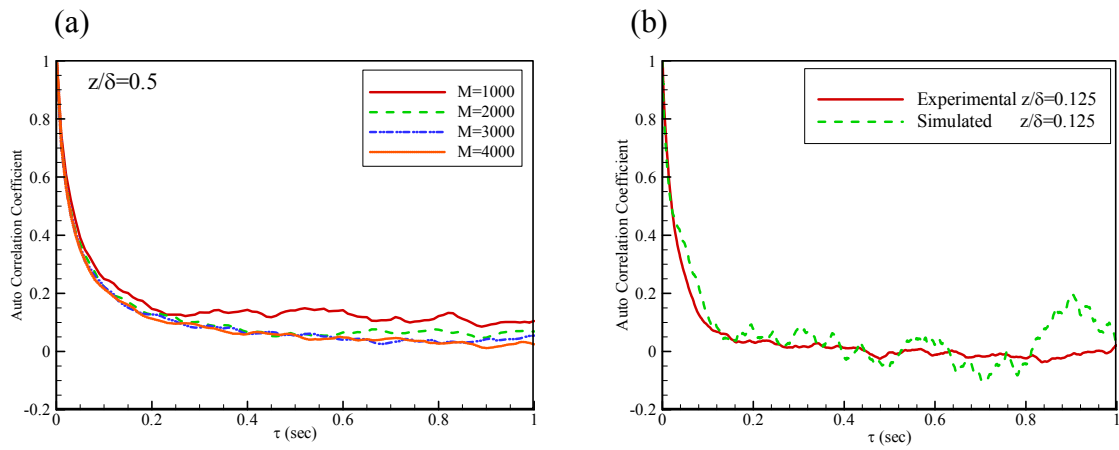


Fig.2 Comparison of auto-correlation coefficients

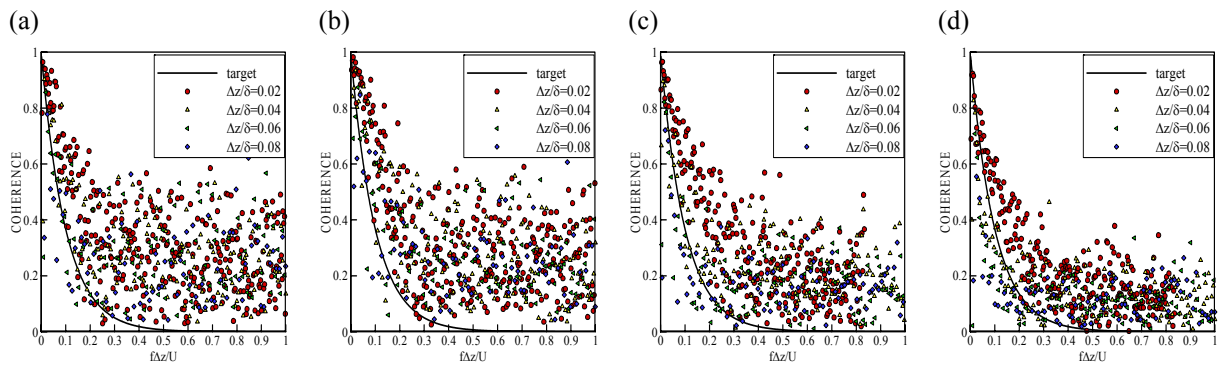


Fig.3 Parameter adjustment at  $z/\delta=0.5$  (a)  $\theta_1=25$ , (b)  $\theta_1=15$ , (c)  $\theta_1=8$ , (d)  $\theta_1=5.5$ .

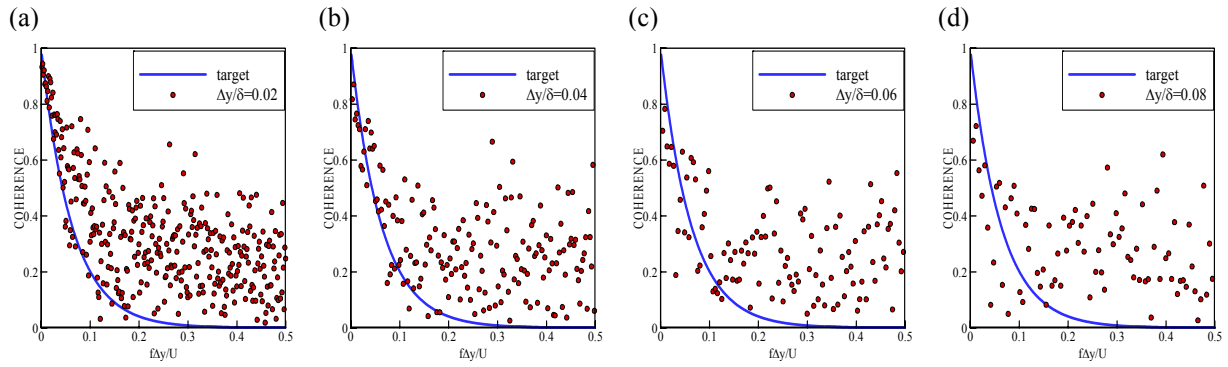


Fig.4 Vertical coherence at  $z/\delta=0.5$  with  $\theta_1=5.5$  (a)  $\Delta y/\delta=0.02$ , (b)  $\Delta y/\delta=0.04$ , (c)  $\Delta y/\delta=0.06$ , (d)  $\Delta y/\delta=0.08$ .

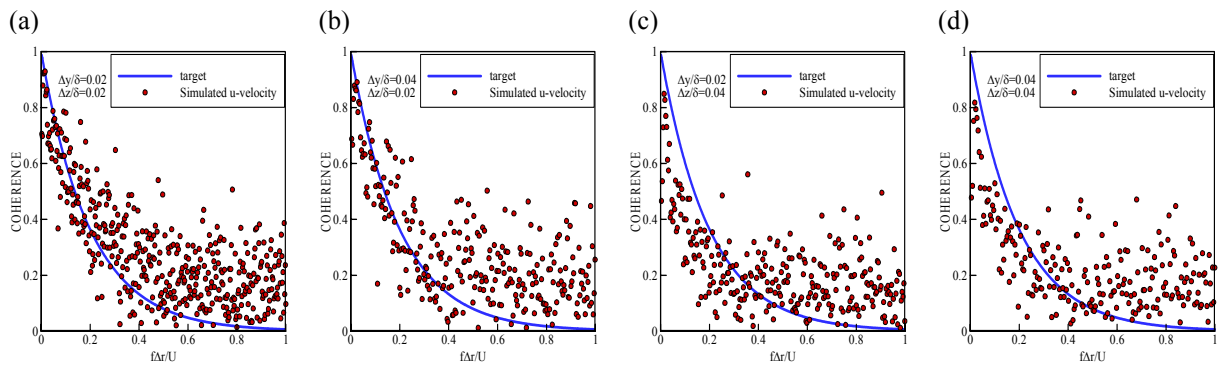


Fig 5. Cross coherence at  $z/\delta=0.5$  with  $\theta_1=5.5$  (a)  $\Delta y/\delta=0.02$   $\Delta z/\delta=0.02$ , (b)  $\Delta y/\delta=0.04$   $\Delta z/\delta=0.02$ , (c)  $\Delta y/\delta=0.02$   $\Delta z/\delta=0.04$ , (d)  $\Delta y/\delta=0.04$   $\Delta z/\delta=0.04$ .

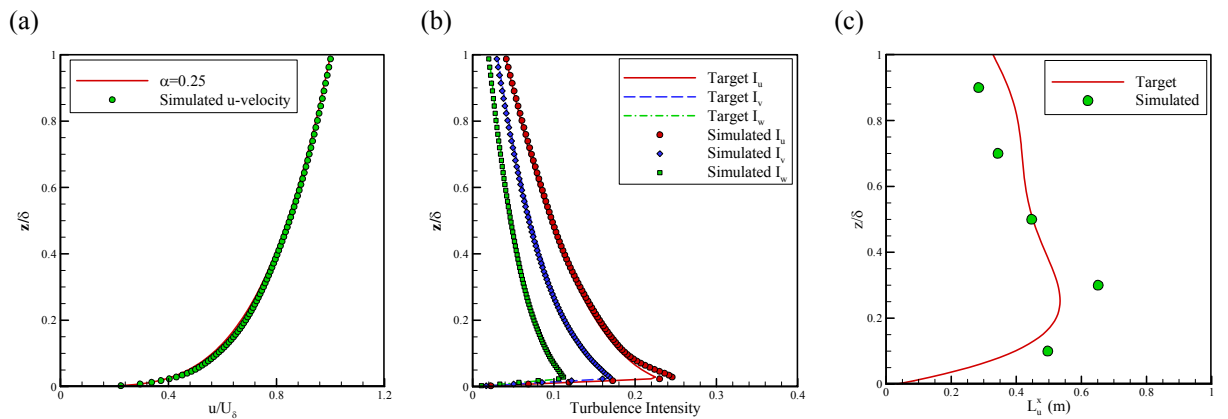


Fig. 6 Comparison of setting and simulated profile (a) mean wind speed, (b) turbulence intensity and (c) integral length scale.

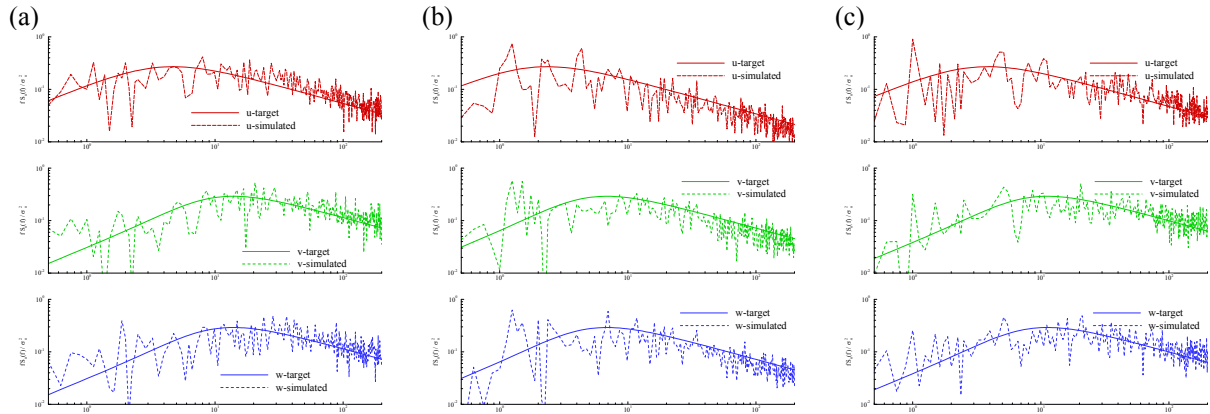


Fig. 7 Spectra generated by MDSRFG and comparison with target spectra at (a)  $z/\delta=0.1$ , (b)  $z/\delta=0.5$  and (c)  $z/\delta=0.75$ .

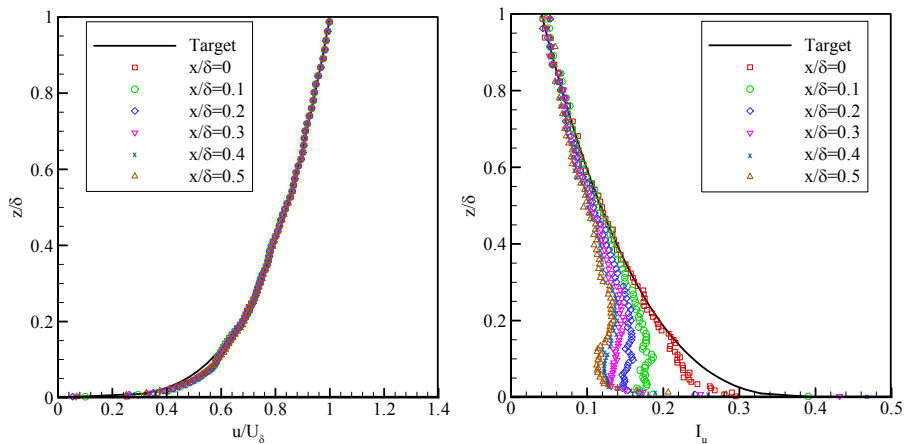


Fig. 8 Comparison of target and simulated profile along the longitude

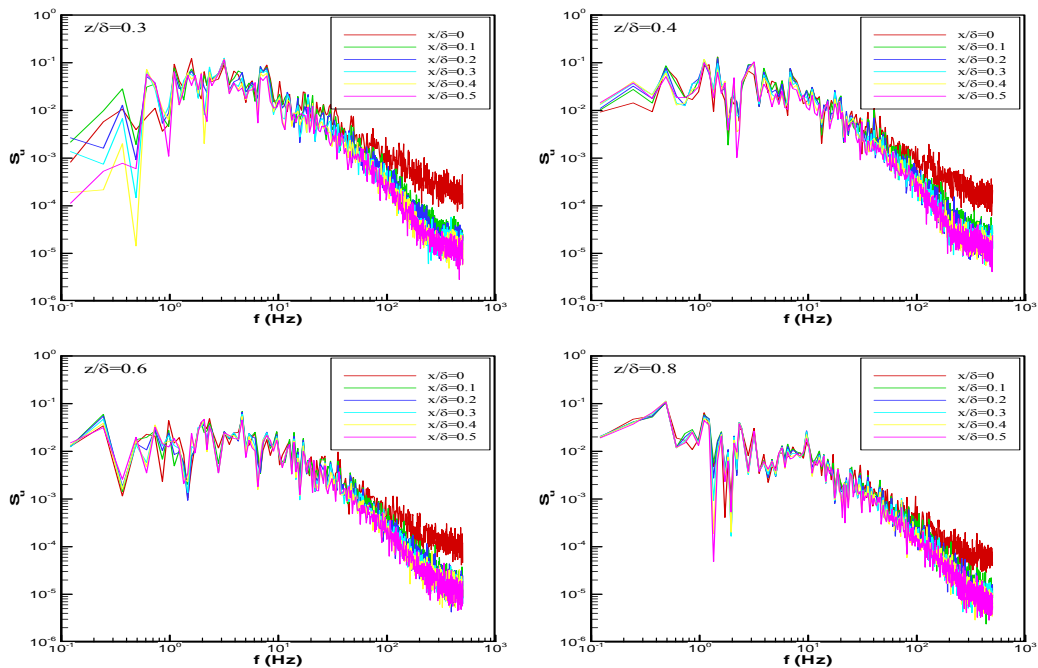


Fig. 9 Comparison of the spectra along longitudinal direction